

Testing Spatial Stationarity and Segmenting Spatial Processes into Stationary Components

ShengLi Tzeng^a, Bo-Yu Chen^b, Hsin-Cheng Huang^{c,*}

^a*Department of Applied Mathematics, National Sun Yat-Sen University, Taiwan.*

^b*Department of Statistics, Purdue University, USA.*

^c*Institute of Statistical Science, Academia Sinica, Taiwan.*

Abstract

In geostatistics, the process of interest is commonly assumed to be stationary in a spatial region, particularly when only a single realization of data at finite locations is available. In this research, we develop a test for stationarity utilizing robust local estimates of spatial covariances. The test statistic is derived from clustering the data locations using Voronoi tessellations. If the stationary assumption is violated, we provide a method to show the nonstationary features by partitioning the region into stationary sub-regions. We further determine the best number of partitions using Bayesian information criterion. The proposed method is computationally efficient and applicable to irregularly spaced data. Its effectiveness is demonstrated through some simulation studies and an application to a precipitation dataset in Colorado.

Keywords: Geostatistics, irregularly spaced data, Monte Carlo test, nonstationary spatial process, spatial clustering, Voronoi tessellation

^{*}Corresponding author

Email address: hchuang@stat.sinica.edu.tw (Hsin-Cheng Huang)

1. Introduction

Consider a spatial process $\{y(\mathbf{s}) : \mathbf{s} \in D\}$ of interest defined on a region $D \subset \mathbb{R}^2$. Suppose that we observe data $\mathbf{z} \equiv (z(\mathbf{s}_1), \dots, z(\mathbf{s}_n))'$ at n spatial locations, which may be irregularly spaced, according to the measurement equation:

$$z(\mathbf{s}_i) = y(\mathbf{s}_i) + \varepsilon(\mathbf{s}_i); \quad i = 1, \dots, n, \quad (1)$$

where $\varepsilon(\mathbf{s}_1), \dots, \varepsilon(\mathbf{s}_n) \sim N(0, \sigma_\varepsilon^2)$ are white-noise variables, representing measurement errors. A major problem in geostatistics, called kriging, is to predict $y(\mathbf{s}_0)$ at any location $\mathbf{s}_0 \in D$ based on \mathbf{z} . For simplicity, we assume that the mean function of the process $y(\cdot)$ is known and, without loss of generality, zero. Then for a given covariance function of $y(\cdot)$, it is well known that the optimal linear predictor of $y(\mathbf{s}_0)$ is

$$\hat{y}(\mathbf{s}_0) = \text{cov}(y(\mathbf{s}_0), \mathbf{z}) \text{var}(\mathbf{z})^{-1} \mathbf{z}. \quad (2)$$

The predictor given by (2) is called the simple-kriging predictor (see Cressie, 1993).

Given a realization of noisy data \mathbf{z} at n locations, the covariance function of $y(\cdot)$ is typically assumed to be stationary. A commonly used stationary covariance model is the isotropic Matérn family (Matérn, 1986) given by

$$C_y(\mathbf{u}; \boldsymbol{\theta}) = \text{cov}(y(\mathbf{s}), y(\mathbf{s} + \mathbf{u})) = \frac{\tau^2}{2^{\nu-1}\Gamma(\nu)} \left(\frac{\sqrt{2\nu}}{\alpha} \|\mathbf{u}\| \right)^\nu \mathcal{K}_\nu \left(\frac{\sqrt{2\nu}}{\alpha} \|\mathbf{u}\| \right); \quad \mathbf{s}, \mathbf{s} + \mathbf{u} \in \mathbb{R}^2, \quad (3)$$

where $\mathcal{K}_\nu(\cdot)$ is the modified Bessel function of the second kind of order ν , τ^2 is a variance parameter, and $\boldsymbol{\theta} \equiv (\alpha, \nu)'$ consists of a scale parameter α and a smoothness parameter ν . However, spatial covariance functions are far away from stationarity in many situations. They are affected by local conditions and vary with topographical features.

Testing spatial stationarity has been proposed before. Fuentes (2005) established a test in the frequency domain. Jun and Genton (2012) provided a general method to test stationarity for spatial and spatio-temporal data, which does not require distributional assumptions.

However, these approaches require data observed on a regular grid. More recently, Bandyopadhyay and Rao (2017) proposed a frequency domain test that can be applied to irregularly spaced locations.

In this paper, we consider a spatial clustering approach using robust local estimates of spatial covariances to test whether the process $y(\cdot)$ is stationary on D . If the stationarity is violated, we further partition D into K components $\{D_1, \dots, D_K\}$ such that each process $\{y(\mathbf{s}) : \mathbf{s} \in D_k\}$ is stationary, for $k = 1, \dots, K$.

The rest of this paper is organized as follows. In Section 2, we develop a statistic to monitor spatial heterogeneity. The statistic is designed for irregularly spaced data using a robust variogram estimate. We then introduce our approach to partition the domain D into K homogeneous subregions using Voronoi tessellations (Voronoi, 1908). Section 3 gives the proposed test for stationarity using a t -type statistic based on the Voronoi cells obtained from Section 2 with $K = 2$. Some simulation results are given in Section 4. An application to a precipitation dataset in Colorado is provided in Section 5. Finally, Section 6 concludes with a summary.

2. Segmenting spatial processes into stationary components

2.1. A statistic for local spatial dependence

First, we construct a statistic to monitor the local spatial dependence of $y(\cdot)$ around \mathbf{s}_i , for $i = 1, \dots, n$. To find local structure around \mathbf{s}_i , we consider a neighborhood set of \mathbf{s}_i :

$$N_i \equiv \{j : \|\mathbf{s}_j - \mathbf{s}_i\| \leq r, j \neq i\}; \quad i = 1, \dots, n, \quad (4)$$

where $\|\cdot\|$ is the Euclidean distance and $r > 0$ is a range parameter. If $y(\cdot)$ is an isotropic stationary process around \mathbf{s}_i , then its variogram at distance h is

$$2\gamma_{y,i}(h) \equiv \text{E}(y(\mathbf{s}) - y(\mathbf{s}_i))^2, \text{ for } h = \|\mathbf{s} - \mathbf{s}_i\| \leq r; \quad i = 1, \dots, n.$$

It follows that for $\mathbf{s} \in N_i$,

$$2\gamma_{z,i}(\|\mathbf{s} - \mathbf{s}_i\|) \equiv \text{E}((z(\mathbf{s}) - z(\mathbf{s}_i))^2) = 2\gamma_y(\|\mathbf{s} - \mathbf{s}_i\|) + 2\delta_{ij}\sigma_\varepsilon^2; \quad i = 1, \dots, n,$$

where $\delta_{ij} \equiv 1$ if $i = j$; 0 otherwise. To reflect the local behavior, it is desirable to consider N_i 's with a small r . To obtain a statistic that is robust to outliers, we utilize a squared-root transform and apply the following approximation formula (Cressie and Hawkins, 1980):

$$\frac{|z(\mathbf{s}_j) - z(\mathbf{s}_i)|^{1/2}}{\{2\gamma_{z,i}(\|\mathbf{s}_j - \mathbf{s}_i\|)\}^{1/4}} \approx \mathcal{N}(2^{1/4}\pi^{-1/2}\Gamma(3/4), 2^{1/2}\{\pi^{-1/2} - \pi^{-1}\Gamma(3/4)^2\}); \quad \mathbf{s}_j \in N_i. \quad (5)$$

Considering the variogram at a short distance to be linear:

$$\gamma_{y,i}(h) = a_i h; \quad h \leq r, i = 1, \dots, n,$$

for some constants $a_i > 0$; $i = 1, \dots, n$, and applying a Taylor expansion to $(2\gamma_{z,i}(h))^{1/4}$ at $h = 0$, we obtain

$$\gamma_{z,i}(h)^{1/4} = (a_i h + \sigma_\varepsilon^2)^{1/4} = (\sigma_\varepsilon^2)^{1/4} + \frac{1}{4}(\sigma_\varepsilon^2)^{-3/4}a_i h + O(h^2); \quad h \leq r, i = 1, \dots, n.$$

Substituting $(\sigma_\varepsilon^2)^{1/4} + \frac{1}{4}(\sigma_\varepsilon^2)^{-3/4}a_i \|\mathbf{s}_j - \mathbf{s}_i\|$ above for $\gamma_{z,i}(\|\mathbf{s}_j - \mathbf{s}_i\|)^{1/4}$ in (5) leads to

$$\mathbb{E}\left(\frac{|z(\mathbf{s}_j) - z(\mathbf{s}_i)|^{1/2} - 2^{1/2}\pi^{-1/2}\Gamma(3/4)(\sigma_\varepsilon^2)^{1/4}}{\|\mathbf{s}_j - \mathbf{s}_i\|}\right) \approx 2^{-3/2}\pi^{-1/2}\Gamma(3/4)(\sigma_\varepsilon^2)^{-3/4}a_i, \quad (6)$$

for $i = 1, \dots, n$. Note that while the left-hand side of (6) depends on \mathbf{s}_j , the right-hand side does not. This motivates us to use the following statistic to monitor the heterogeneity of spatial dependence:

$$\xi_i \equiv \frac{1}{|N_i|} \sum_{j \in N_i} \frac{|z(\mathbf{s}_j) - z(\mathbf{s}_i)|^{1/2} - 2^{1/2}\pi^{-1/2}\Gamma(3/4)(\sigma_\varepsilon^2)^{1/4}}{\|\mathbf{s}_j - \mathbf{s}_i\|}; \quad i \in \mathcal{I}, \quad (7)$$

where $\mathcal{I} \equiv \{i : |N_i| > 0, i = 1, \dots, n\}$, and $|N_i|$ denotes the number of elements in N_i .

2.2. Voronoi tessellations into stationary components

We note from (5) that ξ_i is approximately Gaussian with $\mathbb{E}(\xi_i) \approx 2^{-3/2}\pi^{-1/2}\Gamma(3/4)(\sigma_\varepsilon^2)^{-3/4}a_i$, for $i \in \mathcal{I}$. Let $n^* \equiv |\mathcal{I}|$, and without loss of generality, assume that $\mathcal{I} = \{1, \dots, n^*\}$. Then for a stationary and isotropic process $y(\cdot)$, we have $a_1 = \dots = a_{n^*}$, and hence $\mathbb{E}(\xi_1) \approx \dots \approx \mathbb{E}(\xi_{n^*})$. Therefore, we can apply a spatial-clustering approach to segment D into stationary components based on $\boldsymbol{\xi} \equiv (\xi_1, \dots, \xi_{n^*})'$. In practice, we recommend choosing $r = \{5|D|/(n\pi)\}^{1/2}$ in (4), so that $|N_i| \approx 5$ on average, for $i \in \mathcal{I}$.

Using ξ , we can partition the region D into homogeneous subregions within each the process $y(\cdot)$ is stationary. We employ the Voronoi diagram by considering K seeds $\{\mathbf{p}_1, \dots, \mathbf{p}_K\}$, where $\mathbf{p}_1, \dots, \mathbf{p}_K \in \mathbb{R}^2$. Given $\mathbf{p}_1, \dots, \mathbf{p}_K$, we obtain the corresponding Voronoi tessellation that decompose D into K components D_1, \dots, D_K such that all points in D_k are closer to \mathbf{p}_k than $\{\mathbf{p}_1, \dots, \mathbf{p}_{k-1}, \mathbf{p}_{k+1}, \mathbf{p}_K\}$. Define $n_k \equiv \sum_{i \in \mathcal{I}} I(\mathbf{s}_i \in D_k)$; $k = 1, \dots, K$. Let \mathcal{S}_K be the set of all possible K seeds. To find a desired set of K seeds $\{\mathbf{p}_1, \dots, \mathbf{p}_K\}$ from \mathcal{S}_K , we apply the following objective function:

$$f_K(\mathbf{p}_1, \dots, \mathbf{p}_K; \xi) = \sum_{i=1}^{n^*} \left\{ \log(\hat{v}_k(D_k)) - \log \phi \left(\frac{\xi_i - \bar{\mu}_k(D_k)}{\hat{v}_k(D_k)} \right) \right\}, \quad (8)$$

obtained as the sum of negative Gaussian log-likelihoods over n^* locations, where

$$\bar{\mu}_k(D_k) \equiv \frac{1}{n_k} \sum_{i \in \mathcal{I}: \mathbf{s}_i \in D_k} \xi_i, \quad \text{and} \quad \hat{v}_k^2(D_k) \equiv \frac{1}{n_k} \sum_{i \in \mathcal{I}: \mathbf{s}_i \in D_k} (\xi_i - \bar{\mu}_k(D_k))^2; \quad k = 1, \dots, K,$$

are the maximum likelihood (ML) estimators of the mean and the variance of ξ_i , for $i \in \mathcal{I}$ and $\mathbf{s}_i \in D_k$, and $\phi(\cdot)$ is the probability density function of the standard normal distribution. Given any $K \geq 2$, the proposed partition of D is determined by

$$\{\hat{\mathbf{p}}_1^{(K)}, \dots, \hat{\mathbf{p}}_K^{(K)}\} \equiv \arg \min_{\{\mathbf{p}_1, \dots, \mathbf{p}_K\} \in \mathcal{S}_K} f_K(\mathbf{p}_1, \dots, \mathbf{p}_K; \xi) \quad (9)$$

with the corresponding Voronoi tessellation $\hat{D}_1^{(K)}, \dots, \hat{D}_K^{(K)}$. We propose a simple algorithm to find a heuristic solution of (9). Its pseudo-code is outlined in Algorithm 1.

3. The proposed test for stationarity

We consider the following hypothesis test:

$$H_0: y(\cdot) \text{ is stationary} \quad \text{versus} \quad H_1: y(\cdot) \text{ is not stationary.}$$

Based on the two subregions $\hat{D}_1^{(2)}$ and $\hat{D}_2^{(2)}$ selected by (9) with $K = 2$, we propose the following test statistic based on the two-sample t test:

$$T = \frac{|\bar{\mu}_1(\hat{D}_1^{(2)}) - \bar{\mu}_2(\hat{D}_2^{(2)})|}{\sqrt{\hat{v}_1^2(\hat{D}_1^{(2)})/(\hat{n}_1 - 1) + \hat{v}_2^2(\hat{D}_2^{(2)})/(\hat{n}_2 - 1)}}, \quad (10)$$

Algorithm 1 Find a heuristic solution of (9) for given K based on ξ .

Require:

initial seeds: $\{\mathbf{p}_1, \dots, \mathbf{p}_K\}$ obtained from a deterministic K -means algorithm of Nidheesh *et al.* (2017);

the corresponding Voronoi tessellations, D_1, \dots, D_K .

Ensure:

repeat

for $k \leftarrow 1$ to K **do**

 update \mathbf{p}_k by replacing it from $\{\mathbf{s}_i \in D_k : i = 1, \dots, n^*\}$ such that $f_K(\mathbf{p}_1, \dots, \mathbf{p}_K; \xi)$ is minimized;

 update $\{D_1, \dots, D_K\}$ corresponding to the current seeds $\{\mathbf{p}_1, \dots, \mathbf{p}_K\}$;

end for

until no further reduction of $f_K(\mathbf{p}_1, \dots, \mathbf{p}_K; \xi)$ is possible.

where $\hat{n}_k \equiv \sum_{i=1}^{n^*} I(\mathbf{s}_i \in \hat{D}_k^{(2)})$; $k = 1, 2$. The distribution of T is complicated because there is a selection process involved in obtaining $\hat{D}_1^{(2)}$ and $\hat{D}_2^{(2)}$. So we apply a Monte Carlo (MC) method to find the distribution of T under H_0 . Specifically, we assume that under H_0 , $y(\cdot)$ is a Gaussian process with the isotropic Matérn covariance model of (3). We estimate $\boldsymbol{\theta}$ and τ in (3) by ML. We find the ML estimator of $\boldsymbol{\theta} = (\alpha, \nu)'$ by minimizing the negative log profile likelihood:

$$\hat{\boldsymbol{\theta}} \equiv (\hat{\alpha}, \hat{\nu})' \equiv \arg \min_{\boldsymbol{\theta}} \left\{ \frac{1}{2} \log |\boldsymbol{\Omega}(\boldsymbol{\theta})| + \frac{K}{2} \log \{ \mathbf{z}' \boldsymbol{\Omega}(\boldsymbol{\theta})^{-1} \mathbf{z} \} + \text{constant} \right\}, \quad (11)$$

where $\boldsymbol{\Omega}(\boldsymbol{\theta})$ is an $n \times n$ correlation matrix whose (i, j) -th entry is $\{C(\mathbf{s}_i - \mathbf{s}_j) + \sigma_\varepsilon^2 \delta_{ij}\} / \tau^2$.

Then the ML estimator $\hat{\tau}^2$ of τ^2 is given by:

$$\hat{\tau}^2 \equiv \frac{1}{n} \mathbf{z}' \boldsymbol{\Omega}(\hat{\boldsymbol{\theta}})^{-1} \mathbf{z}. \quad (12)$$

To implement the proposed MC method, first, we simulate data $\mathbf{z}^{(m)}$, for $m = 1, \dots, M$, based on (1) and (3) with $\boldsymbol{\theta}$ and τ replaced by $\hat{\boldsymbol{\theta}}$ in (11) and $\hat{\tau}$ in (12). Next, we compute T_m in (10) based on $\mathbf{z}^{(m)}$. Then the MC p -value of the proposed test is

$$\hat{p} = \frac{1}{M+1} \sum_{m=1}^M I(T_m > T). \quad (13)$$

In practice, we may first perform the stationarity test and obtain the p -value \hat{p} of (13). If $\hat{p} \geq 0.05$, we use a stationary model for subsequent analysis. Otherwise, we apply the

proposed spatial segmentation method to partition D into K stationary subregions with K selected by Bayesian information criterion (BIC) (Schwarz, 1978):

$$\text{BIC}(K) = f_K(\hat{\mathbf{p}}_1^{(K)}, \dots, \hat{\mathbf{p}}_K^{(K)}) + 4K \log(n^*). \quad (14)$$

Specifically, we segment the region into \hat{K} homogeneous components with

$$\hat{K} = \arg \min_{K \in \mathbb{N}} \text{BIC}(K).$$

4. Simulation studies

4.1. Testing stationarity

We examined the size of the proposed stationarity test under H_0 by performing the same simulation experiment as in Section 7.1.1 of Bandyopadhyay and Rao (2017). We considered a zero-mean spatial process $\{y(\mathbf{s}) : \mathbf{s} \in D\}$ on a region $D = [-5/2, 5/2] \times [-5/2, 5/2]$ with a Matérn covariance function of (3). We generated data according to (1) with $\tau^2 = 1$, $\nu = 1/2$, $\alpha \in \{1/3, 2/3, 1, 4/3, 2\}$, and $\sigma_e^2 \in \{0, 0.01\}$. In addition, we considered various sample sizes $n \in \{50, 100, 500, 1000, 2000\}$ and two distributions for sampling locations, including a uniform distribution and a clustered distribution with two clusters (see details in Bandyopadhyay and Rao, 2017), resulting in a total of $5 \times 2 \times 5 \times 2 = 100$ combinations.

We compared our method with BR's (Bandyopadhyay and Rao, 2017). The empirical Type-I error rates under various settings for the uniform and the clustered distributions are shown in Table 1 and Table 2, respectively. Although our method shows a few elevated Type-I error rates when spatial dependence is strong, overall, the Type-I error rates are close to the nominal level. On the other hand, the Type-I error rates for the BR's method tend to be too large for a few cases under the uniform design and too small for many instances under the clustered design. The distributions of p-values for various scenarios are displayed in Figures 1-4. They are all very close to the uniform distribution on $(0, 1)$ as we anticipate.

Next, we investigated the power of the proposed test following the same setups in Bandyopadhyay and Rao (2017). We considered three scenarios. In the first two scenarios, we

n	Method	$\sigma_\epsilon^2 = 0$					$\sigma_\epsilon^2 = 0.01$				
		$\alpha = \frac{1}{3}$	$\alpha = \frac{2}{3}$	$\alpha = 1$	$\alpha = \frac{4}{3}$	$\alpha = 2$	$\alpha = \frac{1}{3}$	$\alpha = \frac{2}{3}$	$\alpha = 1$	$\alpha = \frac{4}{3}$	$\alpha = 2$
50	Ours	0.068	0.054	0.052	0.058	0.060	0.062	0.060	0.056	0.058	0.054
50	BR	0.030	0.020	0.040	0.050	0.090	0.030	0.020	0.050	0.050	0.080
100	Ours	0.034	0.042	0.044	0.054	0.058	0.034	0.046	0.044	0.056	0.050
100	BR	0.030	0.030	0.030	0.040	0.040	0.030	0.050	0.040	0.050	0.040
500	Ours	0.046	0.054	0.056	0.052	0.050	0.040	0.050	0.048	0.054	0.048
500	BR	0.020	0.030	0.020	0.030	0.030	0.040	0.080	0.070	0.130	0.120
1000	Ours	0.072	0.072	0.068	0.070	0.054	0.072	0.072	0.070	0.070	0.068
1000	BR	0.050	0.050	0.060	0.060	0.080	0.080	0.100	0.100	0.140	0.130
2000	Ours	0.078	0.066	0.064	0.064	0.072	0.074	0.074	0.068	0.076	0.080
2000	BR	0.070	0.060	0.090	0.090	0.080	0.070	0.090	0.090	0.180	0.180

Table 1: Empirical Type-I errors for our method and BR’s method (Bandyopadhyay and Rao, 2017) under various scenarios with a uniform sampling design based on 500 simulated replicates.

n	Method	$\sigma_\epsilon^2 = 0$					$\sigma_\epsilon^2 = 0.01$				
		$\alpha = \frac{1}{3}$	$\alpha = \frac{2}{3}$	$\alpha = 1$	$\alpha = \frac{4}{3}$	$\alpha = 2$	$\alpha = \frac{1}{3}$	$\alpha = \frac{2}{3}$	$\alpha = 1$	$\alpha = \frac{4}{3}$	$\alpha = 2$
50	ours	0.064	0.060	0.074	0.072	0.078	0.058	0.06	0.070	0.076	0.072
50	BR	0.020	0.020	0.010	0.010	0.020	0.020	0.020	0.020	0.030	0.020
100	ours	0.082	0.074	0.072	0.062	0.054	0.08	0.078	0.064	0.074	0.068
100	BR	0.020	0.020	0.020	0.020	0.020	0.020	0.030	0.020	0.030	0.030
500	ours	0.060	0.052	0.058	0.060	0.056	0.064	0.052	0.052	0.060	0.060
500	BR	0.020	0.020	0.010	0.010	0.010	0.010	0.020	0.020	0.010	0.010
1000	ours	0.056	0.058	0.064	0.066	0.060	0.060	0.060	0.060	0.062	0.062
1000	BR	0.010	0.010	0.010	0.010	0.010	0.010	0.010	0.010	0.010	0.020
2000	ours	0.052	0.062	0.074	0.076	0.076	0.058	0.058	0.072	0.074	0.076
2000	BR	0.010	0.010	0.010	0.010	0.010	0.010	0.010	0.010	0.010	0.010

Table 2: Empirical Type-I errors for our method and BR’s method (Bandyopadhyay and Rao, 2017) under various scenarios with a clustered sampling design based on 500 simulated replicates.

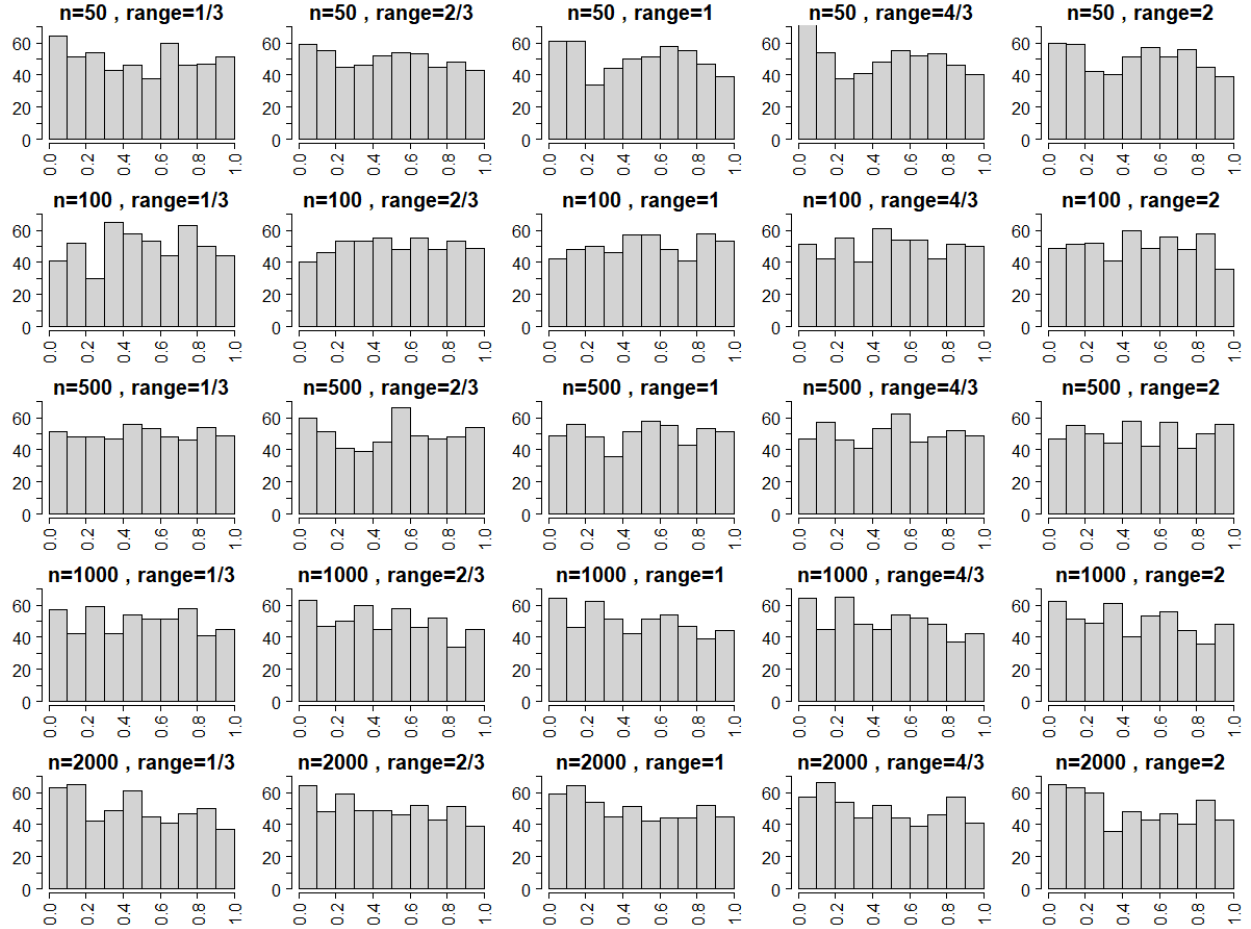


Figure 1: The distributions of p-values under H_0 for various scenarios with $\sigma_\epsilon^2 = 0$ under a uniform sampling design.

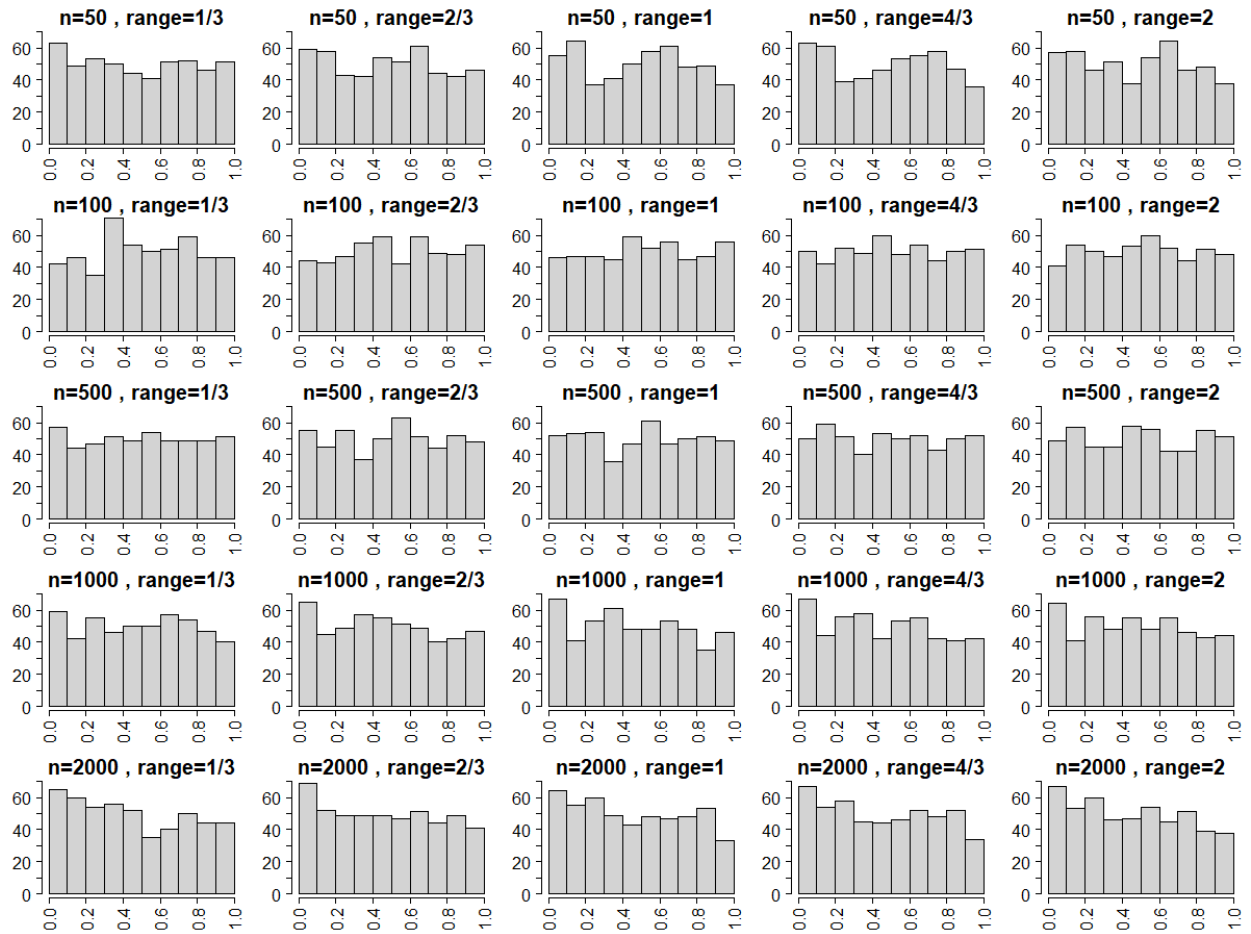


Figure 2: The distributions of p-values under H_0 for various scenarios with $\sigma_\epsilon^2 = 0.01$ under a uniform sampling design.

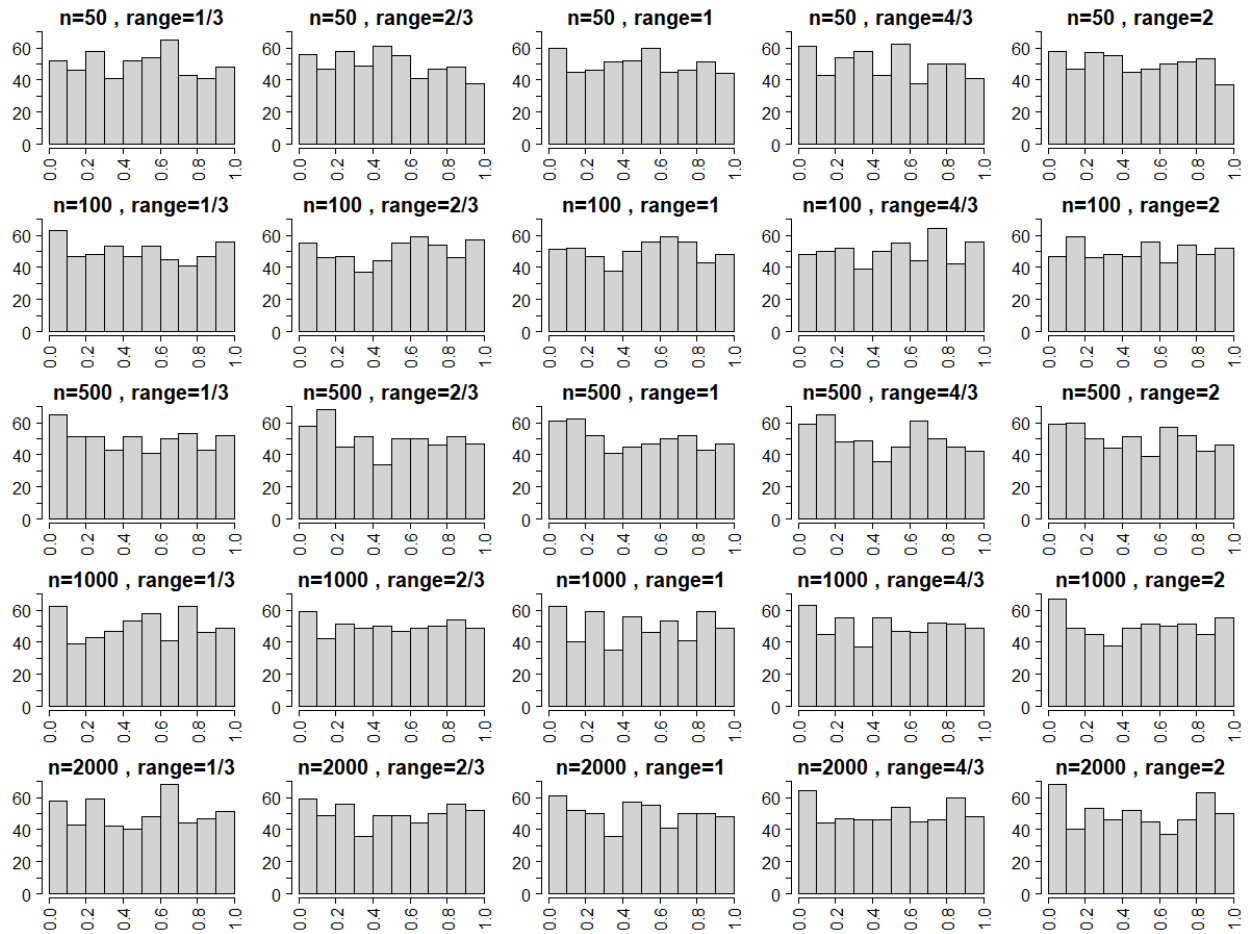


Figure 3: The distributions of p-values under H_0 for various scenarios with $\sigma_\epsilon^2 = 0$ under a clustered sampling design.

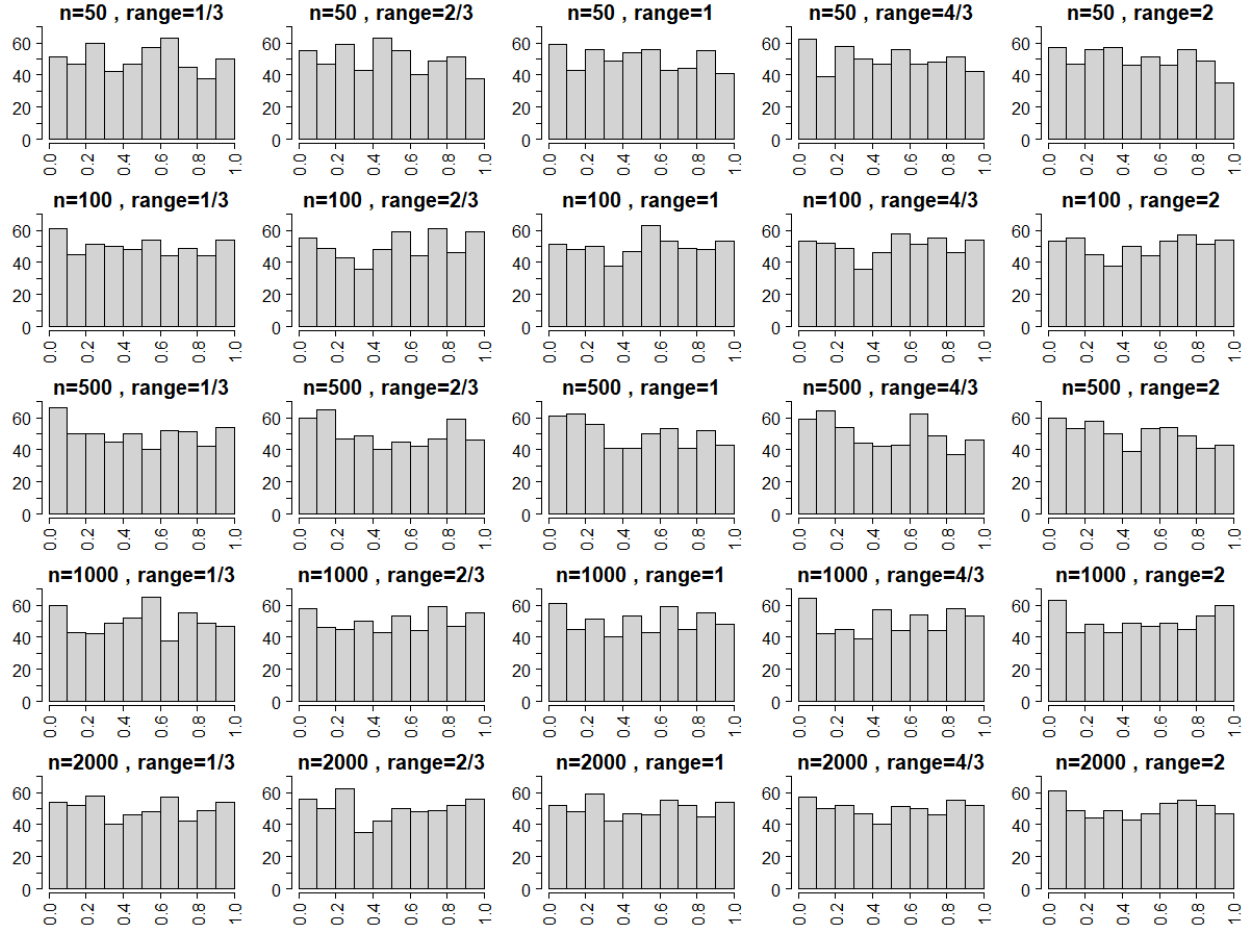


Figure 4: The distributions of p-values under H_0 for various scenarios with $\sigma_\epsilon^2 = 0.01$ under a clustered sampling design.

n	Method	$\sigma_\epsilon^2 = 0$			$\sigma_\epsilon^2 = 0.01$		
		$\lambda = 20$	$\lambda = 40$	4 blocks	$\lambda = 20$	$\lambda = 40$	4 blocks
50	Our	0.050	0.058	0.074	0.054	0.060	0.076
50	BR	0.020	0.030	0.050	0.030	0.040	0.050
100	Our	0.060	0.044	0.106	0.058	0.048	0.100
100	BR	0.050	0.040	0.040	0.040	0.040	0.040
500	Our	0.340	0.136	0.570	0.328	0.140	0.548
500	BR	0.190	0.100	0.110	0.180	0.090	0.110
1000	Our	0.760	0.266	0.926	0.744	0.264	0.910
1000	BR	0.470	0.350	0.240	0.460	0.360	0.240
2000	Our	0.990	0.570	1.000	0.980	0.560	1.000
2000	BR	0.700	0.850	0.360	0.710	0.850	0.360

Table 3: Empirical powers for our and BR's methods (Bandyopadhyay and Rao, 2017) under various scenarios based on 500 simulated replicates.

replaced the stationary Matérn covariance function of (3) by a nonstationary Matérn covariance function with $\lambda = 20$ and 40, respectively:

$$C_y(\mathbf{s}_1, \mathbf{s}_2) = |\Sigma_\lambda(\mathbf{s}_1)|^{1/4} |\Sigma_\lambda(\mathbf{s}_2)|^{1/4} |\{\Sigma_\lambda(\mathbf{s}_1) + \Sigma_\lambda(\mathbf{s}_2)\}/2|^{-1/2} \exp(-\sqrt{Q_\lambda(\mathbf{s}_1, \mathbf{s}_2)}), \quad (15)$$

where

$$Q_\lambda(\mathbf{s}_1, \mathbf{s}_2) \equiv 2(\mathbf{s}_1 - \mathbf{s}_2)' \{ \Sigma_\lambda(\mathbf{s}_1) + \Sigma_\lambda(\mathbf{s}_2) \}^{-1} (\mathbf{s}_1 - \mathbf{s}_2),$$

$$\Sigma_\lambda(\mathbf{s}) \equiv \begin{pmatrix} \log\left(\frac{s_x}{\lambda} + \frac{3}{4}\right) & -\frac{\|\mathbf{s}\|^2}{\lambda^2} \\ \frac{\|\mathbf{s}\|^2}{\lambda^2} & \log\left(\frac{s_x}{\lambda} + \frac{3}{4}\right) \end{pmatrix} \begin{pmatrix} 1 & 0 \\ 0 & 0.5 \end{pmatrix} \begin{pmatrix} \log\left(\frac{s_x}{\lambda} + \frac{3}{4}\right) & \frac{\|\mathbf{s}\|^2}{\lambda^2} \\ -\frac{\|\mathbf{s}\|^2}{\lambda^2} & \log\left(\frac{s_x}{\lambda} + \frac{3}{4}\right) \end{pmatrix},$$

and $\mathbf{s} = (s_x, s_y)'$. For the third scenario, we considered a zero-mean piecewise stationary process $\{y(\mathbf{s}) : \mathbf{s} \in D\}$ by dividing $D = [-5/2, 5/2] \times [-5/2, 5/2]$ into 2×2 blocks of equal sizes. The processes on four blocks are mutually independent and have the Matérn covariance functions of (3), with $\tau^2 = 1$, $\nu = 1/2$, and four different values of $\alpha \in \{1, 1/3, 1/2, 2/3\}$ for the four blocks. For each scenario, we considered the uniform sampling design and generated data according to (1) with $\sigma_\epsilon^2 \in \{0, 0.01\}$ and $n \in \{50, 100, 500, 1000, 2000\}$, resulting in 10 different combinations. The empirical powers are displayed in Table 3 based on 500 simulated replicates. Except for a few case in Scenario 2 with $\gamma = 40$ and $n \geq 1000$, our method outperforms the BR's method by having more power.

4.2. Spatial segmentation

We examined the proposed method in spatial segmentation. We considered a region $D = [0, 1]^2$ and decomposed it into $D_1 \cup D_2$ as shown in Figure 5. We generated a zero-mean spatial process $\{y(\mathbf{s}) : \mathbf{s} \in D\}$ on D based on

$$y(\mathbf{s}) = w_1(\mathbf{s}; a)\eta_1(\mathbf{s}) + w_2(\mathbf{s}; a)\eta_2(\mathbf{s}); \quad \mathbf{s} \in D, \quad (16)$$

where

$$w_k(\mathbf{s}; a) \equiv \frac{\exp(-d(\mathbf{s}, D_k)/a)}{\exp(-d(\mathbf{s}, D_1)/a) + \exp(-d(\mathbf{s}, D_2)/a)}; \quad \mathbf{s} \in D, k \in \{1, 2\},$$

are weight functions with $a > 0$ controlling the degree of smoothness for process $y(\cdot)$ around the boundary between D_1 and D_2 , $d(\mathbf{s}, D_k) \equiv \min_{\mathbf{s}^* \in D_k} \|\mathbf{s} - \mathbf{s}^*\|$, and $\boldsymbol{\eta}(\mathbf{s}) \equiv (\eta_1(\mathbf{s}), \eta_2(\mathbf{s}))'$ is a zero-mean bivariate spatial process with a bivariate exponential covariance function:

$$\text{cov}(\eta_k(\mathbf{s}), \eta_{k'}(\mathbf{s}^*)) = \left(\frac{2\alpha_k \alpha_{k'}}{\alpha_k^2 + \alpha_{k'}^2} \right)^{1/2} \exp \left(- \frac{(\alpha_k^2 + \alpha_{k'}^2)^{1/2}}{2^{1/2} \alpha_k \alpha_{k'}} \|\mathbf{s} - \mathbf{s}^*\| \right); \quad k, k' \in \{1, 2\}.$$

We generated data according to (1) and (16) with $\sigma_\varepsilon^2 = 0$, $\alpha_1 = 0.1$, and $\alpha_2 \in \{0.1, 0.2, 0.3, 0.4, 0.5\}$. Additionally, we considered $n \in \{100, 500\}$ and $a \in \{0.01, 0.1\}$, resulting in a total of 20 combinations. Note that α_2 controls the degree of non-stationarity. When $\alpha_1 = \alpha_2$, we obtain $y(\cdot)$ to be a stationary process with $\text{cov}(y(\mathbf{s}), y(\mathbf{s}^*)) = \exp(-\|\mathbf{s} - \mathbf{s}^*\|/\alpha_1)$ regardless of the value of a . By contrast, a larger departure of α_2 from α_1 indicates a higher degree of non-stationarity. These features can be seen in Figure 6, which shows realizations of $y(\cdot)$ with $\alpha_2 \in \{0.1, 0.2, 0.3, 0.4, 0.5\}$.

We applied the proposed method of (9) to segment D into Voronoi subregions $\{\hat{D}_1, \dots, \hat{D}_K\}$. We selected the final K according to BIC of (14). The performance of an estimated clustering $\tilde{\mathcal{D}} = \{\tilde{D}_1, \dots, \tilde{D}_K\}$ is evaluated using the Rand index (Rand, 1971) based on $\{\mathbf{s}_1, \dots, \mathbf{s}_n\}$:

$$R(\mathcal{D}, \tilde{\mathcal{D}}) \equiv \frac{n_{00} + n_{11}}{n_{00} + n_{01} + n_{10} + n_{11}},$$

where $\mathcal{D} = \{D_1, D_2\}$ is the true clustering,

n_{00} is the number of point pairs that are in different clusters under both \mathcal{D} and $\tilde{\mathcal{D}}$,

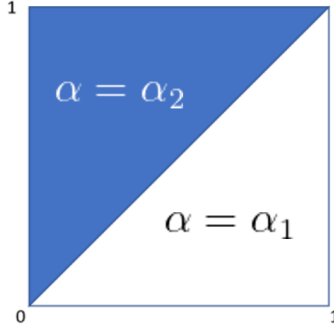


Figure 5: A partition of D into D_1 and D_2 and their corresponding spatial dependence parameters α_1 and α_2 .

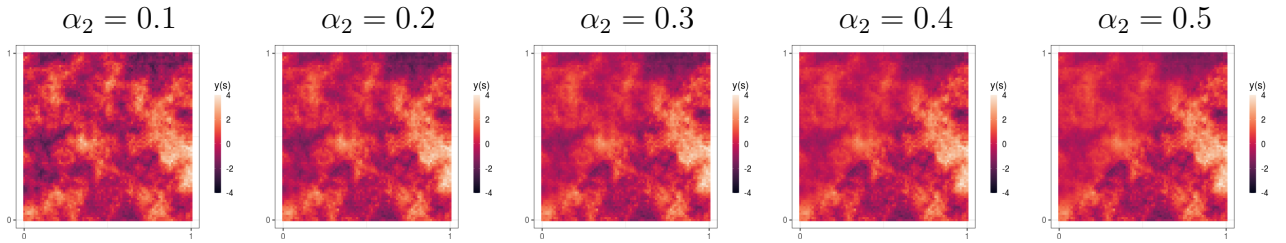


Figure 6: Realizations of $y(\cdot)$ from models with various α_2 values, where a larger α_2 value corresponds to a higher degree of nonstationarity, and $\alpha_2 = 0.1$ corresponds to a stationary process.

n_{01} is the number of point pairs that are in the same cluster under \mathcal{D} but in different clusters under $\tilde{\mathcal{D}}$,

n_{10} is the number of point pairs that are in different clusters under \mathcal{D} but in the same cluster under $\tilde{\mathcal{D}}$,

n_{11} is the number of point pairs that are in the same cluster under both \mathcal{D} and $\tilde{\mathcal{D}}$.

α_2	$a = 0.01$		$a = 0.1$	
	$n = 100$	$n = 500$	$n = 100$	$n = 500$
0.1	0.326	0.296	0.286	0.266
0.2	0.446	0.736	0.402	0.636
0.3	0.560	0.800	0.474	0.724
0.4	0.642	0.794	0.580	0.706
0.5	0.694	0.834	0.648	0.660

Table 4: Proportions of selecting the correct number (i.e., $K = 2$) of clusters under various situations based on 500 simulated replicates.

α_2	$a = 0.01$		$a = 0.1$	
	$n = 100$	$n = 500$	$n = 100$	$n = 500$
0.1	0.563	0.547	0.556	0.544
0.2	0.603	0.746	0.582	0.663
0.3	0.650	0.845	0.609	0.748
0.4	0.689	0.884	0.660	0.778
0.5	0.735	0.905	0.686	0.793

Table 5: Average Rand index values based on the number of clusters selected by BIC under various situations based on 500 simulated replicates.

5. An application to precipitation data in Colorado

In this section, we applied our method to a precipitation dataset in Colorado. The dataset can be obtained from the Geophysical Statistics Project at the National Center for Atmospheric Research (<http://www.image.ucar.edu/GSP/Data/US.monthly.met/CO.html>), which has been analyzed previously by Paciorek and Schervish (2006) and Qadir *et al.* (2021). It consists of monthly total precipitation (in mm) recorded at 367 weather stations across the state of Colorado from 1895 to 1997. It is well known that Western Colorado is mountainous with larger topographical variability than Eastern Colorado.

Following Qadir *et al.* (2021), we considered the cumulative precipitations in the year 1992 and analyzed the data observed at 254 stations with no missing observations after applying the log transformation. Figure 7(a) shows the precipitation data we analyzed.

Applying the proposed test of (10) described in Section 3, we obtained a p-value smaller than 0.01 for testing spatial stationarity, suggesting that the underlying process is likely nonstationary. We then segmented the process into stationary processes on subregions by applying the proposed spatial segmentation method of (9) introduced in Section 2.2. From (14), we obtained the BIC values 260.6, 185.8, 181.2, and 205.1 for $K = 1, \dots, 4$, respectively. The smallest BIC value is achieved at $K = 3$. Figure 7(b)-(d) shows the segmentation results based on $K = 2, 3, 4$. Even though we did not utilize any additional information (such as elevation) other than precipitations, Colorado Eastern Plains, which tend to have a different climate pattern from the rest, are automatically segmented as a subregion for $K \in \{2, 3, 4\}$,

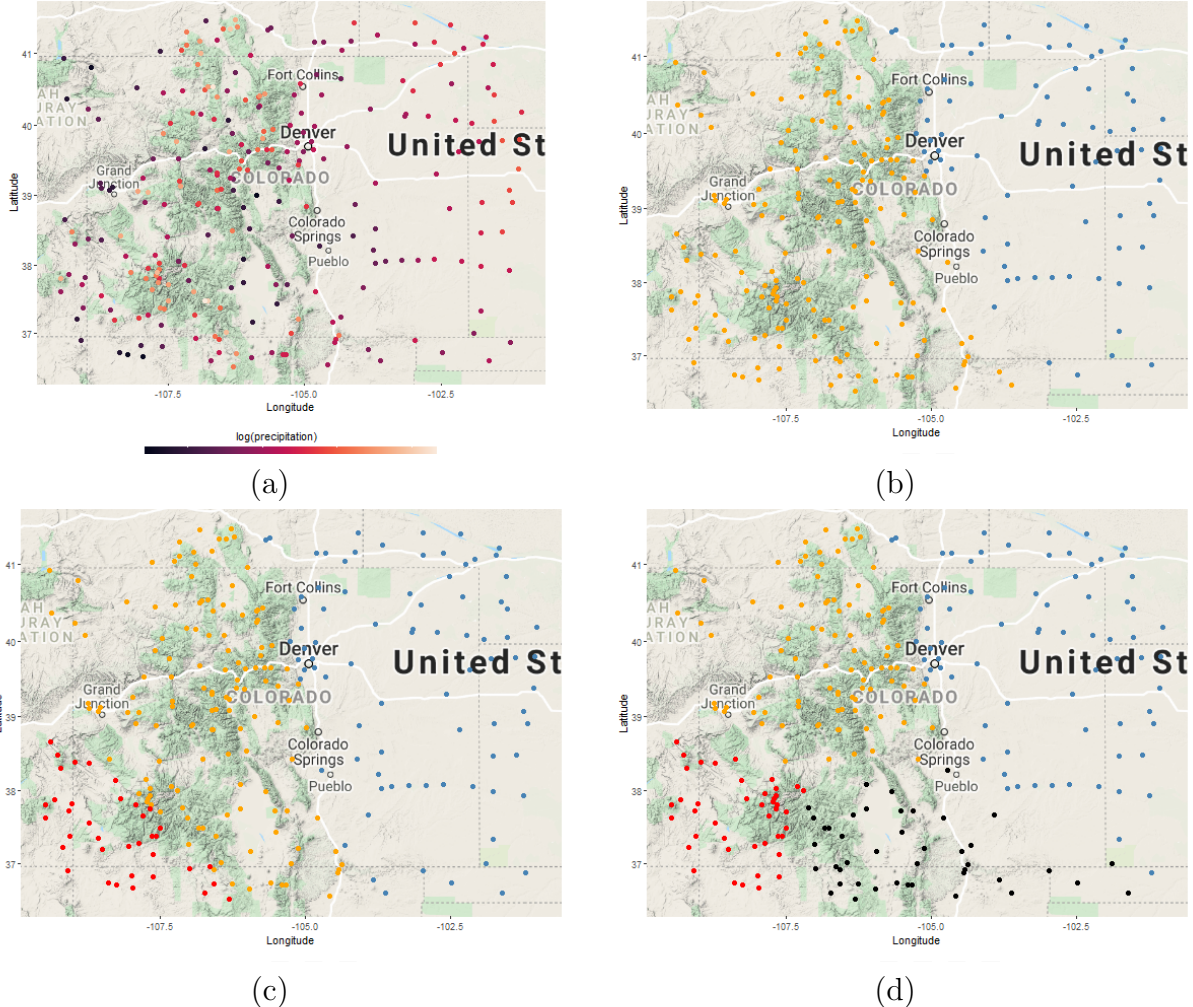


Figure 7: (a) Precipitation amounts (mm in log scale) at 254 stations in Colorado in 1992; (b) Two subregions obtained by the proposed methods; (c) Three subregions obtained by the proposed methods; (d) Four subregions obtained by the proposed methods.

demonstrating that the proposed spatial segmentation method is effective.

6. Summary

We propose a novel test to detect the nonstationarity of a spatial process. Our test is designed for data observed at irregularly spaced locations with no repeated measurements. It is computationally efficient, properly controls the Type-I error rate, and is more powerful than existing methods. Compared to the test of Bandyopadhyay and Rao (1997), which tends to perform worse (and has better control of the Type-I error rate) under an irregular sampling design, our test is not much affected by how irregular the data are located.

The proposed stationarity test has another advantage; it can display where the nonstationarity occurs once rejected because we can check the stationary components partitioned by the proposed method. Then we could perform kriging by applying a stationary model on each component separately or go one step further to establish a divide-and-conquer strategy to combine the results. These appear to be promising research directions, particularly when there are massive amounts of spatial data. Further investigations along these lines, including constructing nonstationary models based on locally stationary processes and developing scalable methods for kriging, are of great interest but beyond the scope of this paper. We will develop them elsewhere.

References

Bandyopadhyay, S. and Rao, S. S. (2017). A test for stationarity for irregularly spaced spatial data, *Journal of Royal Statistical Society, Series B*, **79**, 95–123.

Cressie, N. (1993). Statistics for Spatial Data, rev. edn, Wiley, New York, NY.

Cressie, N. and Hawkins, D. M. (1980). Robust estimation of the variogram: I, *Mathematical Geology*, **12**, 115–125.

Fuentes, M. (2005). A formal test for non-stationarity of spatial stochastic processes. *Journal of Multivariate Analysis*, **96**, 30–54.

Jun, M. and Genton, M. (2012) A test for stationarity of spatio-temporal random fields on planar and spherical domains, *Statistica Sinica*, **22**, 1737–1764.

Matérn, B. (1986). *Spatial Variation*, 2nd ed., Springer-Verlag, Berlin.

Nidheesh, N., Nazeer, K. A., and Ameer, P. M. (2017). An enhanced deterministic K-Means clustering algorithm for cancer subtype prediction from gene expression data. *Computers in biology and medicine*, **91**, 213-221.

Paciorek, C. J. and Schervish, M. J. (2006). Spatial modelling using a new class of nonstationary covariance functions. *Environmetrics*, **17**, 483–506.

Qadir, G. A., Sun, Y. and Kurtek, S. (2021). Estimation of spatial deformation for nonstationary processes via variogram alignment. *Technometrics*, **63**, 548–561.

Rand, W. M. (1971). Objective criteria for the evaluation of clustering methods, *Journal of the American Statistical Association*, **66**, 846–850.

Schwarz, G. (1978). Estimating the dimension of a model, *The Annals of Statistics*, **6**, 461–464.

Voronoi, G. (1908). Nouvelles applications des paramètres continus à la théorie des formes quadratiques. Premier mémoire. Sur quelques propriétés des formes quadratiques positives parfaites, *Journal für die reine und angewandte Mathematik (Crelles Journal)*, **1908**, 97–102.